Electronic Supplementary Information (ESI)

Systematic study of ionic conduction in silver iodide / mesoporous alumina composites 2: Effect of silver bromide doping

Yoko Fukui,[a] Yukihiro Yoshida,*[b] Hiroshi Kitagawa[b] and Yohei Jikihara[a]*

[a] NBC Meshtec Inc., 2-50-3 Toyoda, Hino, Tokyo 191-0053, Japan

[b] Division of Chemistry, Graduate School of Science, Kyoto University, Kitashirakawa-Oiwakecho, Sakyo-ku, Kyoto 606-8502, Japan

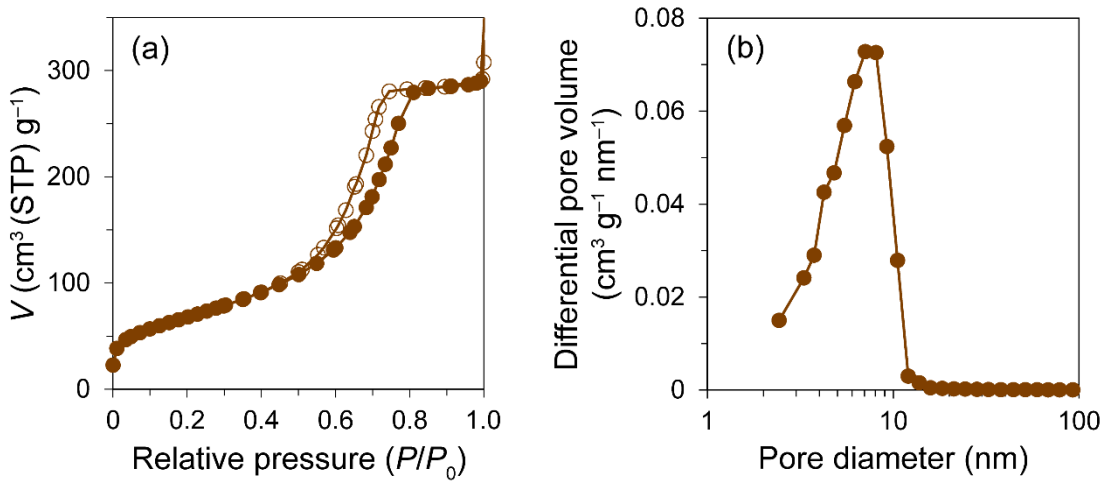

Fig. S1 (a) N_2 gas adsorption (closed circles) and desorption (open circles) isotherms of MPA at 77 K. (b) Pore size distribution of MPA obtained by applying the BJH method.

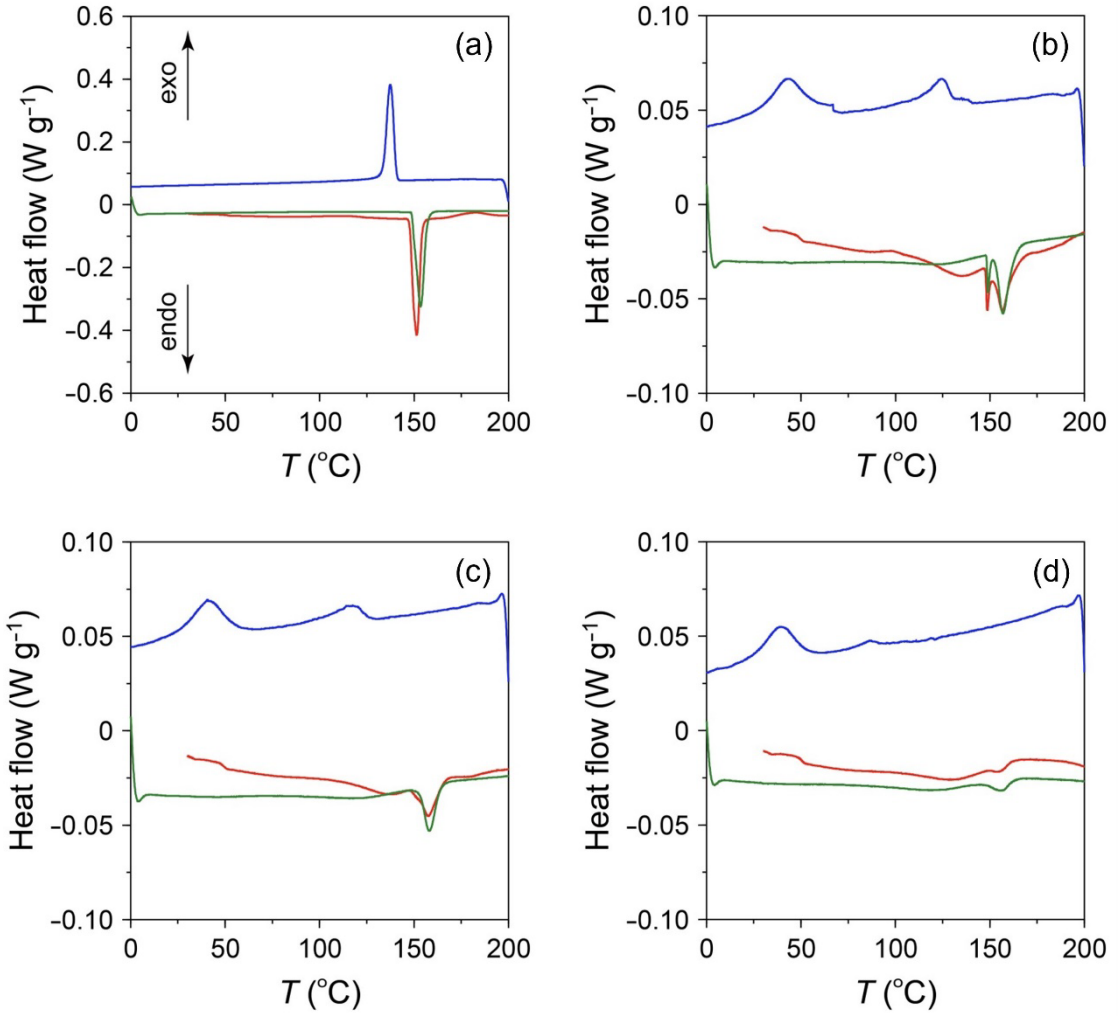

Fig. S2 DSC profiles of **Br0** before heat treatment (a) and after heat treatment at (b) 400 °C, (c) 500 °C, and (d) 600 °C (red: 1st heating process, blue: 1st cooling process, green: 2nd heating process) (see Y. Fukui *et al.*, *Phys. Chem. Chem. Phys.* 2023, **25**, 25594–25602).

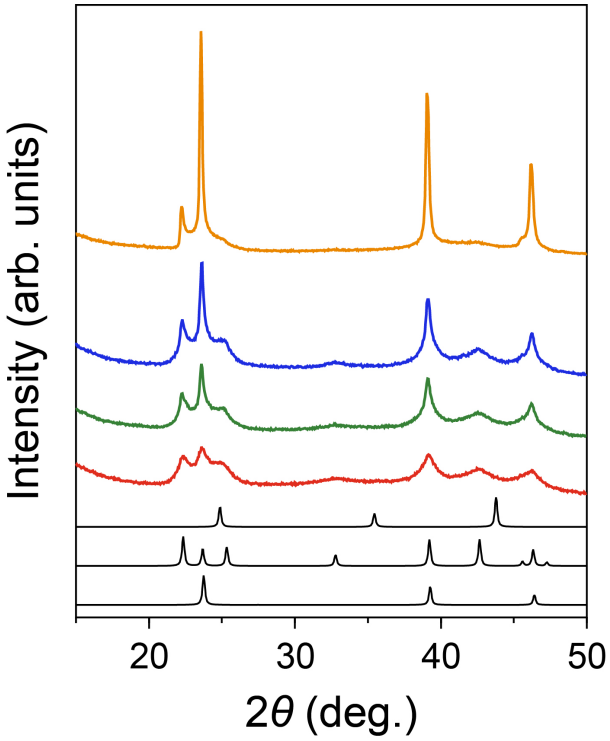

Fig. S3 PXRD patterns of **Br0** (orange: before heat treatment, blue: heat treatment at 400 °C, green: heat treatment at 500 °C, red: heat treatment at 600 °C) along with simulated patterns (black thin lines) of α-, β-, and γ-AgI (from the top) (see Y. Fukui *et al.*, *Phys. Chem. Chem. Phys.* 2023, **25**, 25594–25602).

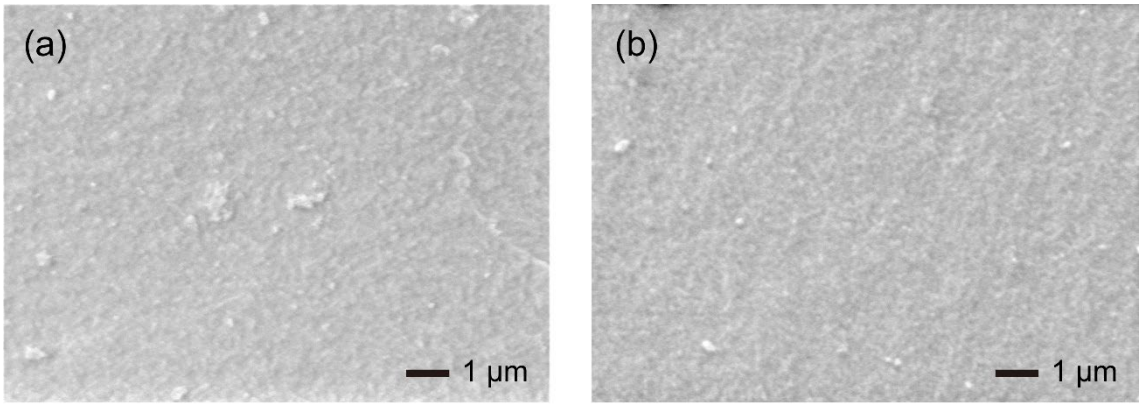

Fig. S4 SEM images of **Br10** (a) before and (b) after heat treatment at 600 °C for 20 h.

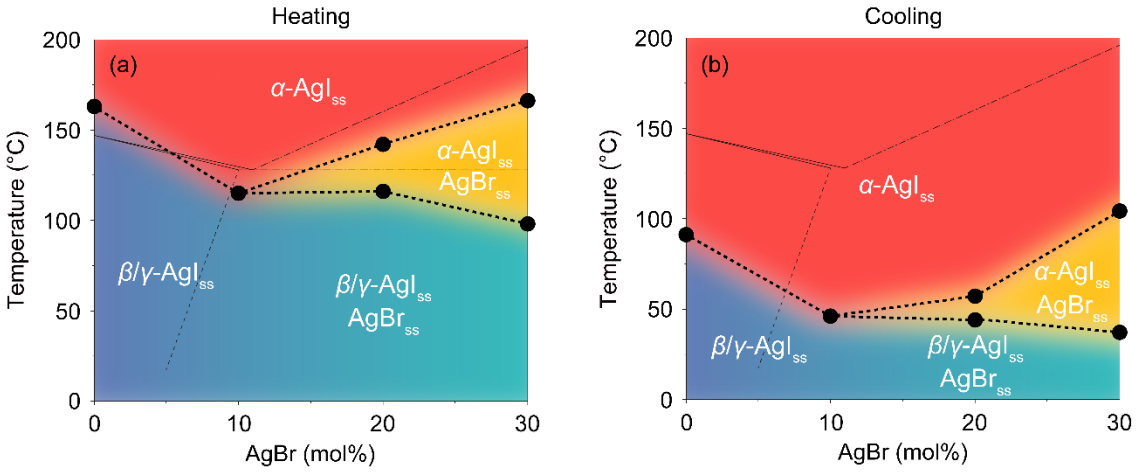

Fig. S5 Phase diagram of AgI-AgBr/MPA system (blue: β/γ-AgI$_{ss}$, green: β/γ-AgI$_{ss}$ + AgBr$_{ss}$, yellow: α-AgI$_{ss}$ + AgBr$_{ss}$, red: α-AgI$_{ss}$). The phase boundaries indicated by black dotted lines were defined when the molar ratio of β/γ-AgI$_{ss}$ or AgBr$_{ss}$ phase reaches 50% relative to that at 30 °C in (a) heating and (b) cooling processes (black circles). The ratios were determined by the Rietveld analysis of the variable-temperature PXRD patterns. The thin black lines represent the phase diagram of bulk AgI-AgBr system (H. Takahashi *et al.*, *Solid State Ionics*, 1984, **14**, 107–112).

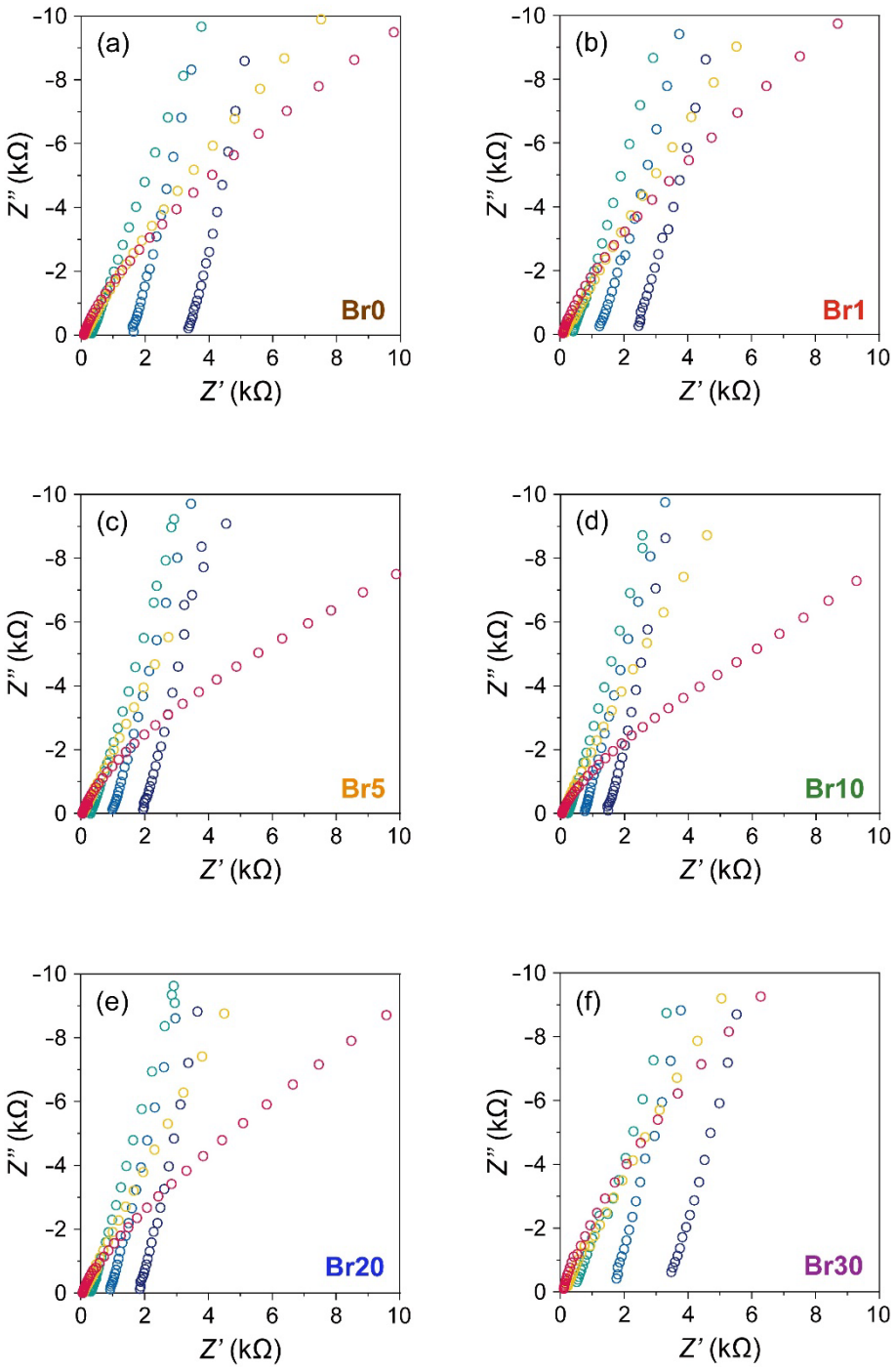

Fig. S6 Temperature dependence of Nyquist plots of AgI-AgBr/MPA composites with various AgI:AgBr molar ratios ((a) **Br0**, (b) **Br1**, (c) **Br5**, (d) **Br10**, (e) **Br20**, and (f) **Br30)** at 25 °C (deep blue), 50 °C (light blue), 100 °C (green), 150 °C (yellow), and 200 °C (red) in the heating process.

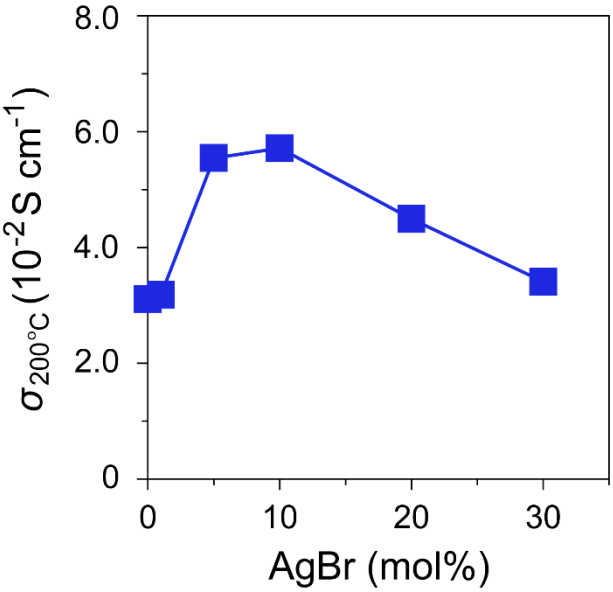

Fig. S7 Plots of $\sigma_{200^{\circ}C}$ against AgBr-doping ratio for AgI-AgBr/MPA composites.

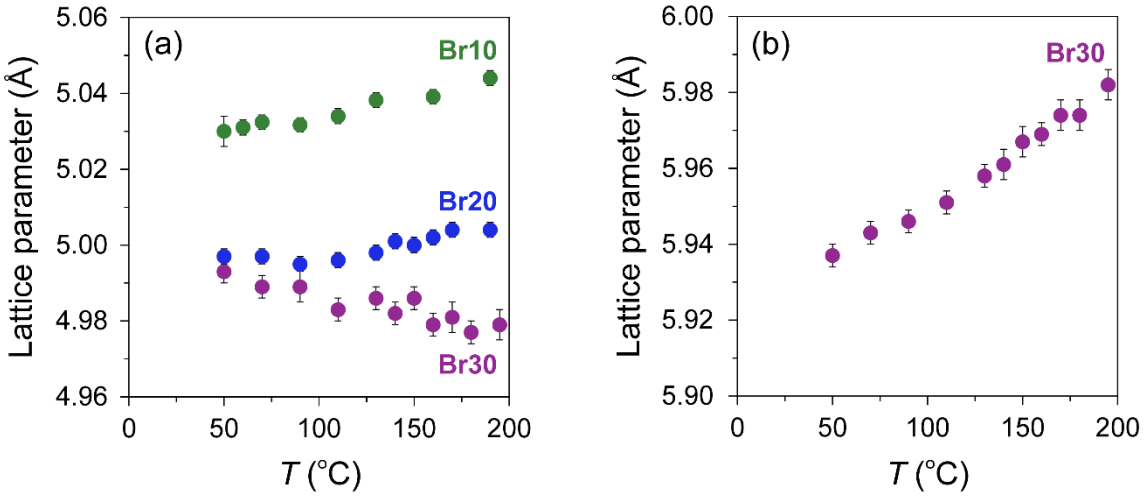

Fig. S8 Temperature dependence of the lattice parameters of (a) cubic α-AgI_{ss} phase in **Br10** (green), **Br20** (blue), and **Br30** (purple) and (b) cubic $AgBr_{ss}$ phase in **Br30** determined by the Rietveld analysis of the variable-temperature PXRD patterns in the cooling process.

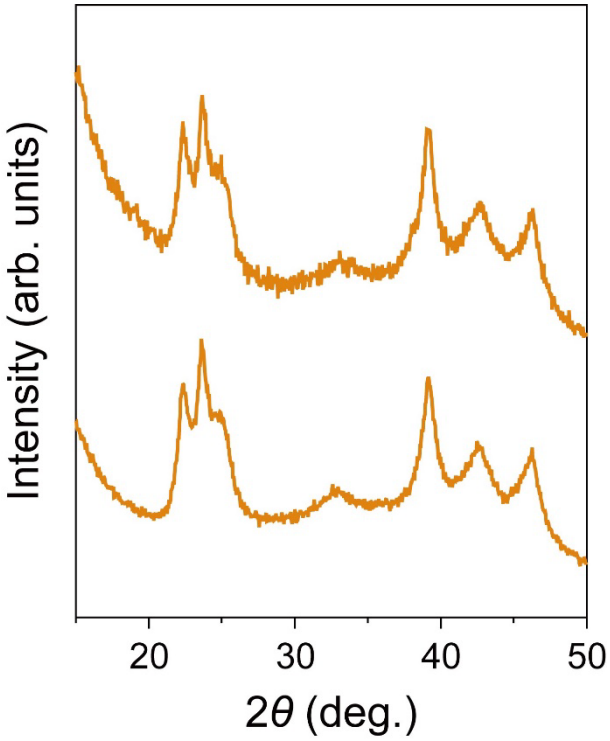

Fig. S9 PXRD patterns of **Br0** before (bottom) and after (top) the electrochemical impedance spectroscopy measurements (25–200 °C) (see Y. Fukui *et al.*, *Phys. Chem. Chem. Phys.* 2023, **25**, 25594–25602).

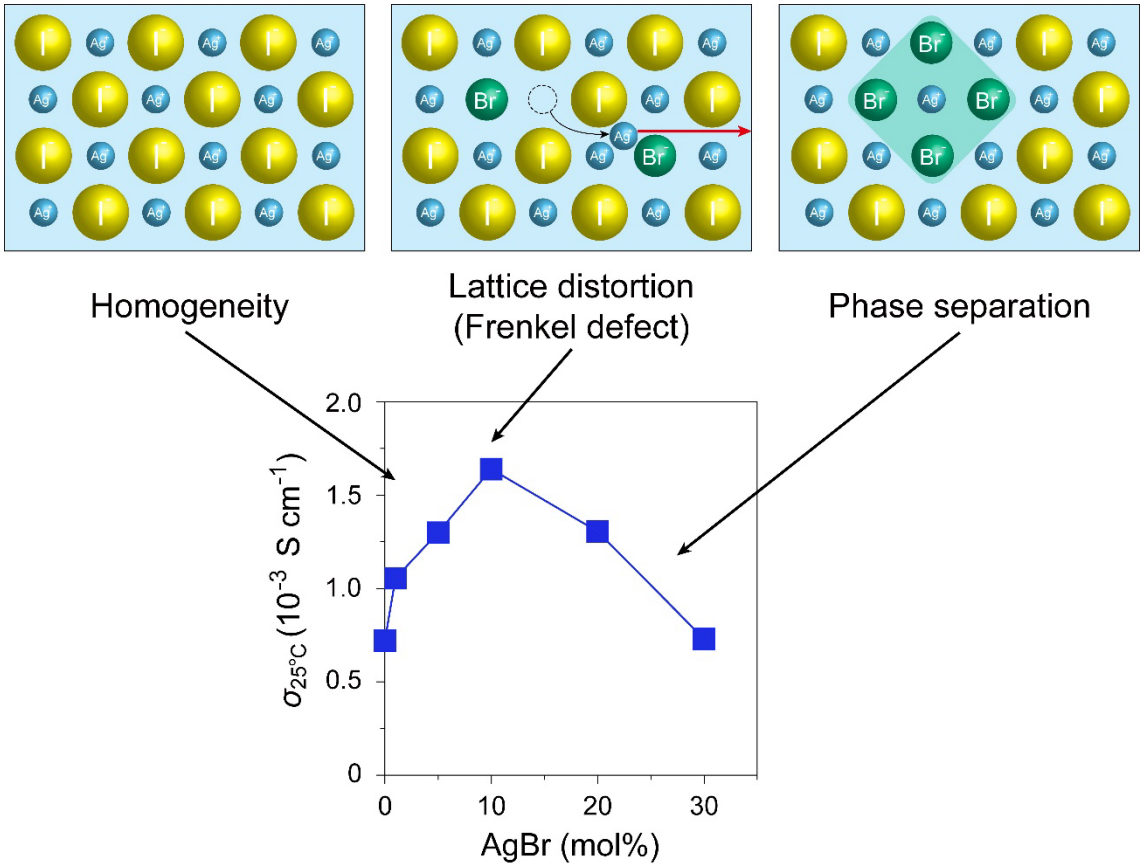

Fig. S10 Schematic illustrations to explain the Ag^+-ion conducting behaviour of AgI-AgBr/MPA composites by varying the AgBr content.

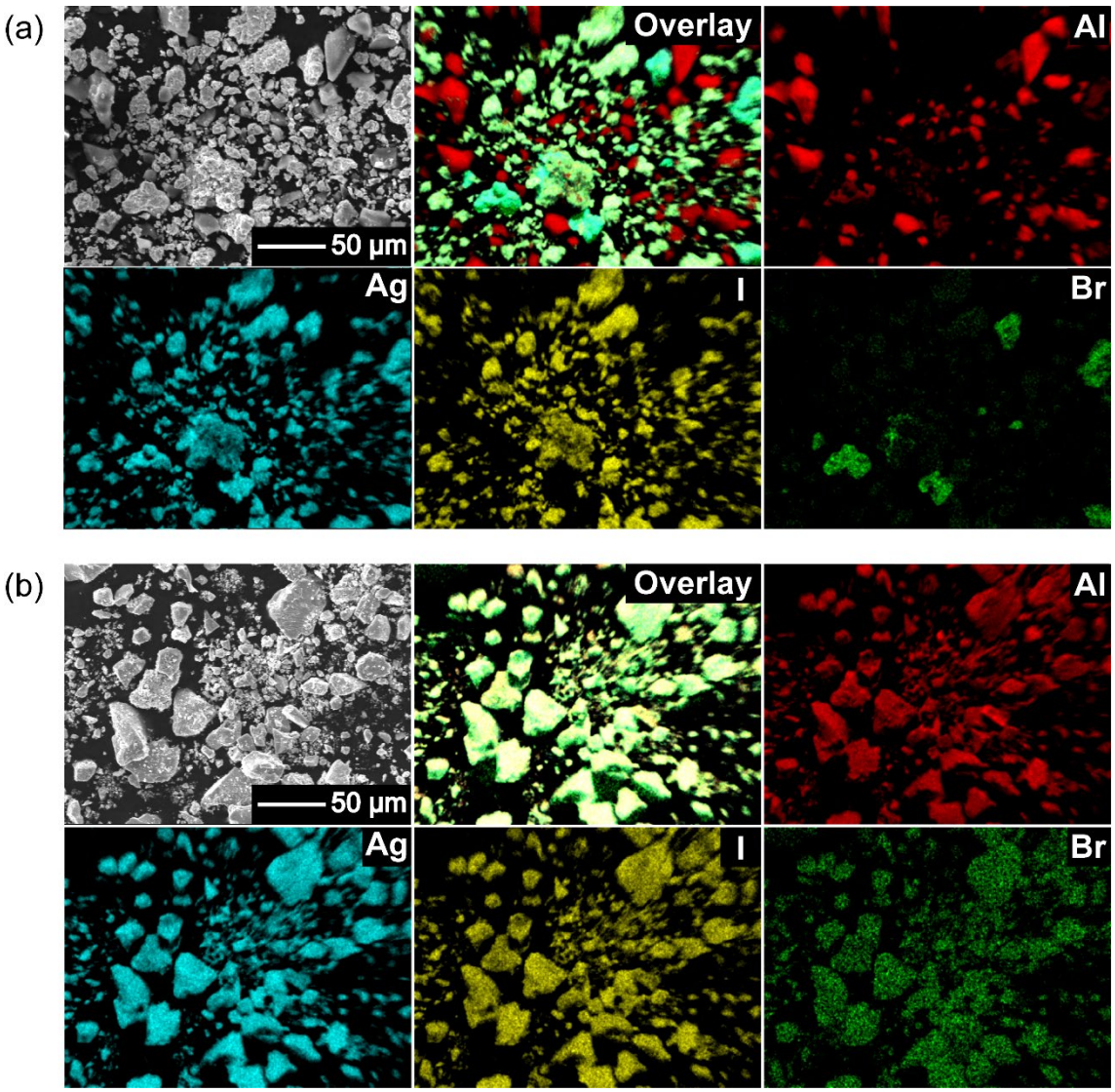

Fig. S11 SEM images and EDS mappings (Overlay, Al, Ag, I, and Br) of **Br20** (a) before and (b) after heat treatment at 600 °C for 20 h.

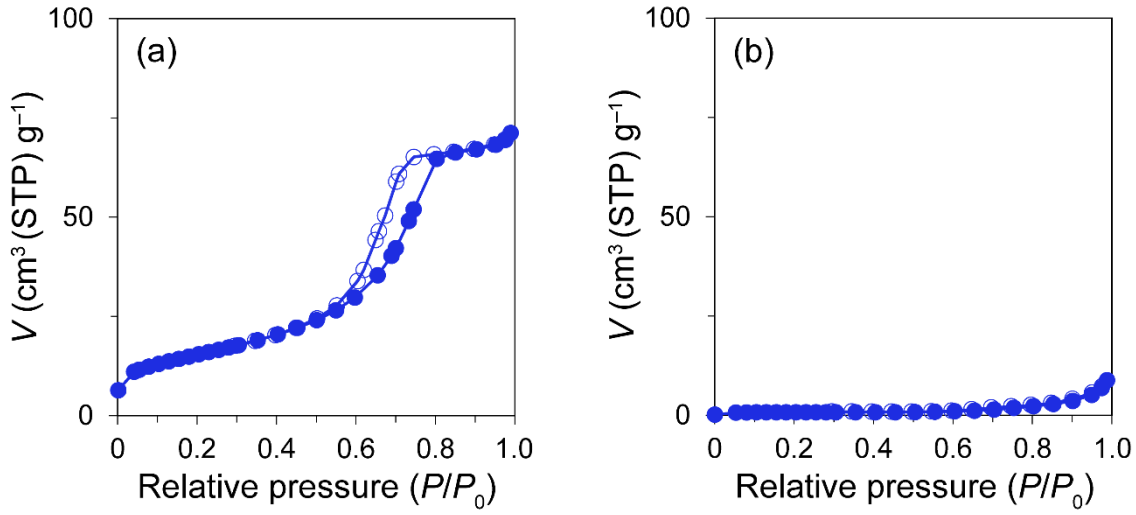

Fig. S12 N_2 gas adsorption (closed circles) and desorption (open circles) isotherms of **Br20** (a) before and (b) after heat treatment at 600 °C for 20 h.

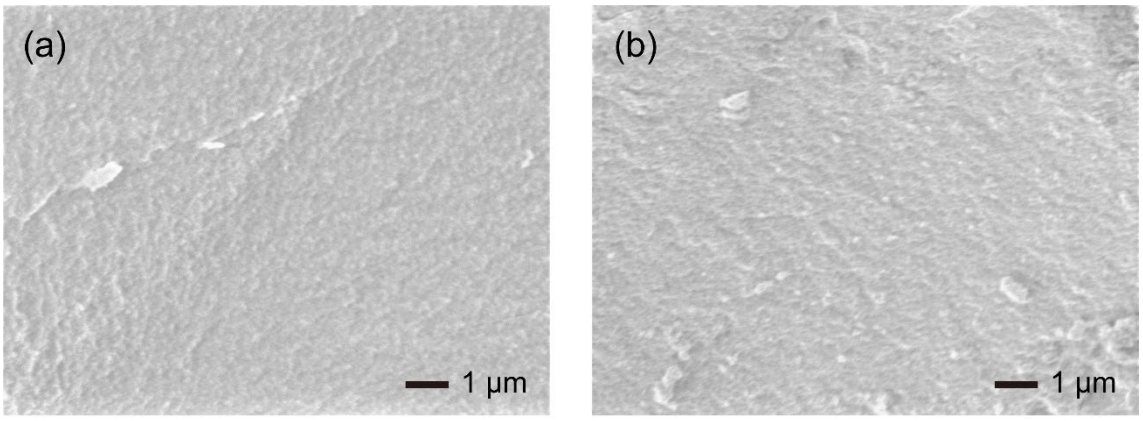

Fig. S13 SEM images of **Br20** (a) before and (b) after heat treatment at 600 °C for 20 h.